Quantum dot-doped silica nanoparticles as probes for targeting of T-lymphocytes

Massimo Bottini[1,2,4]
Federica D'Annibale[2]
Andrea Magrini[2]
Fabio Cerignoli[1]
Yutaka Arimura[1]
Marcia I Dawson[1]
Enrico Bergamaschi[5]
Nicola Rosato[3]
Antonio Bergamaschi[1]
Tomas Mustelin[1]

[1]Burnham Institute for Medical Research, La Jolla, CA, USA; [2]NAST and Department of Environmental, Occupational and Social Medicine, University of Rome Tor Vergata, Rome, Italy; [3]NAST and Department of Experimental Medicine and Biochemical Sciences, University of Rome Tor Vergata, Rome, Italy; [4]INFN, Laboratori Nazionali di Frascati, Frascati, Italy; [5]Department of Clinical Medicine, Nephrology and Health Sciences, University of Parma, Parma, Italy

Abstract: To enhance diagnostic or therapeutic efficacy, novel nanomaterials must be engineered to function in biologically relevant environments, be visible by conventional fluorescent microscopy, and have multivalent loading capacity for easy detection or effective drug delivery. Here we report the fabrication of silica nanoparticles doped with quantum dots and superficially functionalized with amino and phosphonate groups. The amino groups were acylated with a water-soluble biotin-labeling reagent. The biotinylated nanoparticles were subsequently decorated with neutravidin by exploiting the strong affinity between neutravidin and biotin. The resultant neutravidin-decorated fluorescent silica nanoparticles stably dispersed under physiological conditions, were visible by conventional optical and confocal fluorescent microscopy, and could be further functionalized with macromolecules, nucleic acids, and polymers. We also coated the surface of the nanoparticles with biotinylated mouse anti-human CD3 (αCD3). The resultant fluorescent nanoassembly was taken up by Jurkat T cells through receptor-mediated endocytosis and was partially released to lysosomes. Thus, quantum dot-doped silica nanoparticles decorated with neutravidin represent a potentially excellent scaffold for constructing specific intracellular nanoprobes and transporters.

Keywords: silica nanoparticles, neutravidin, surface functionalization, endocytosis, intracellular nanoprobe

Introduction

The emerging field of nanomedicine is aimed at the preservation and improvement of human health using the tools and knowledge of nanotechnology and may lead to the development of more effective means for diagnosing and treating malignancies as compared with current methods. To enhance diagnostic or therapeutic efficacy, novel nanoassemblies must be engineered to function in biologically relevant environments and have multivalent loading capacity to facilitate detection or effective drug delivery. In the past decade, several types of nanoparticles have been prepared and evaluated for tissue targeting, sensing and imaging, and localized therapy (Akerman et al 2002; Salem et al 2003; Bianco 2004; Haag 2004; Langer and Tirrell 2004; Bottini et al 2006a; Shenoy et al 2006). Often, the chemistry of these nanoparticles has limited their stepwise assembly into multilayered systems and their capacity to interact multivalently with cell membrane receptors.

Silica nanoparticles (SNP) have been widely used for biosensing and catalytic applications due to their large surface area to volume ratio, easy fabrication and capacity for doping and/or functionalization with fluorescent molecules (Bottini et al 2006b), magnetic nanoparticles (Wang et al 2005), or semiconducting nanocrystals (Lin et al 2006). SNP can be prepared using several methods, including the popular Stobër (Stobër et al 1968) and the water-in-oil nanoemulsion (Bagwe et al 2004) techniques. The former employs simple hydrolysis of a silica precursor in ethanolic-ammonium hydroxide medium while the latter uses water droplets in reverse micelles as nanoreactors

Correspondence: Massimo Bottini
Burnham Institute for Medical Research, 10901 North Torrey Pines Road, La Jolla, CA 92037, USA
Tel +1 858 646 3100 x3063
Email mbottini@burnham.org

to regulate nanosphere size which is dependent on water droplet dimension, ie, molar ratios of water to surfactant and the precursor, molar ratio of precursor to catalyst, precursor reactivity, and reaction time and temperature.

Quantum dots (QD) are colloidal semiconducting nanocrystals that have diameters of a few nanometers and are typically coated with functionalized polymers that permit the surface tethering of various small and macro-molecules that are compatible with an aqueous environment. Because of their small size, QD energy levels are quantized so that photon energy emission is restricted to a narrow range after broad range absorption. Their quantum behavior is superior to that of small organic fluorescent molecules, which can only fluoresce after excitation within a narrow absorption range and bleach rapidly. Therefore, QD represent an excellent building block for intracellular nanoprobes and delivery systems. However, QD have caused in vitro toxic effects that depend on such factors as dose, size, and chemical functionalization (Hardman 2006). Their solubilization under physiological conditions and superficial functionalization are not straightforward. However encapsulation of QD by SNP has been found to increase their hydrophilicity and decrease their cytotoxicity (Zhang et al 2006). In this regard, SNP encapsulation offers the advantage that specific functional groups can be easily introduced on their surface to reduce aggregation and permit further functionalization to obtain nanoassemblies (Bagwe et al 2006).

In this report we describe the construction and characterization of SNP doped with QD and decorated with neutravidin (Nav). To demonstrate that this fluorescent nanoassembly could be further functionalized with small or macromolecules, we coated its surface with biotinylated mouse anti-human CD3 (αCD3) by exploiting the strong affinity between biotin and Nav. We next investigated the uptake of the resultant QD-SNP-Nav-αCD3 nanoassembly into human Jurkat T cells through receptor-mediated endocytosis. Thus, this nanoassembly represents a potentially excellent scaffold for constructing specific intracellular nanoprobes.

Materials and methods

Materials

Unless otherwise noted, reagent-grade chemicals were used without further purification, and Millipore water was used for all aqueous solutions. Cyclohexane, Triton X-100, n-hexanol, tetramethyl orthosilicate (tmos), (3-aminopropyl)trimetho xysilane (apts), (3-trihydroxy)silylpropyl methylphosphonate (thpmp), ammonium hydroxide (28% NH_3 in water), poly-L-lysine, formaldehyde, dimethyl formamide (DMF), and phosphate-buffered saline (PBS) were purchased from Sigma-Aldrich (St. Louis, MO). ZnS-covered CdSe QD were capped by (trioctyl)phosphine oxide (TOPO) had a 542-nm emission wavelength and a diameter of approximately 2 nm and were obtained from Evident Technologies, Inc. (Troy, NY). The water-soluble biotin-labeling reagent sulfosuccinimidyl-6-(biotin-amido)hexanoate (sulfo-NHS-LC-biotin) and neutravidin (Nav, molecular weight approximately 6×10^4) were purchased from Pierce Biotechnology, Inc. (Rockford, IL). Biotinylated and nonconjugated αCD3 antibodies (molecular weight approximately 1.5×10^5) were from eBioscience, Inc. (San Diego, CA); rabbit anti-human CD107A (LAMP-1) antibody was a gift from Prof. Minoru Fukuda (Burnham Institute for Medical Research, La Jolla, CA). Texas Red-labeled goat anti-rabbit antibody and Texas Red-labeled concanavalin A were from Molecular Probes (Invitrogen Corp., Carlsbad, CA); normal mouse serum (NMS) was from Santa Cruz Biotechnology (Santa Cruz, CA); normal goat serum (NGS) was from Gibco (Invitrogen Corp., Carlsbad, CA); fetal bovine serum (FBS) was from Tissue Culture Biologicals (Informagen, Inc., Newington, NH); RPMI-1640 cell culture medium and Dulbecco's modified Eagle's medium-high glucose (DMEM-HG) were from Cellgro (Mediatech, Inc., Herndon, VA).

Preparation of QD-SNP-Nav

Unless otherwise stated all incubations were done at room temperature. A mixture of cyclohexane, Triton X-100, and n-hexanol (volume ratio 4.2:1:1; 24.8-ml final volume) was converted to a nanoemulsion by stirring at room temperature for 1 h before water (940 µl) and tmos (100.5 µl) were added. This mixture was sonicated for 1 h to facilitate the diffusion of tmos into the encapsulated water droplets. A drop (59 µl) of 28% aqueous ammonium hydroxide was added to catalyze the hydrolysis and condensation of tmos and the mixture was stirred for 30 min. Next, 25 nmoles of QD in toluene (100 µl) were added. The reaction mixture was stirred for 24 h before tmos (10 µl) was added, followed by a mixture of apts (5.9 µl) and thpmp (15.1 µl) 30 min later. This mixture was stirred for 24 h. The QD-doped SNP (QD-SNP, Scheme 1[I]) were precipitated by acetone (25 ml). The precipitate (approximately 25 mg of nanoparticles) was washed several times with water, followed by anhydrous ethanol. A 1 mg aliquot of QD-SNP and 30 mg of sulfo-NHS-LC-biotin were stirred for 2 hours in phosphate buffered saline (PBS, 2 ml). The biotinylated nanoparticles (QD-SNP-bio, Scheme 1[II]) were washed three times with PBS and then incubated with

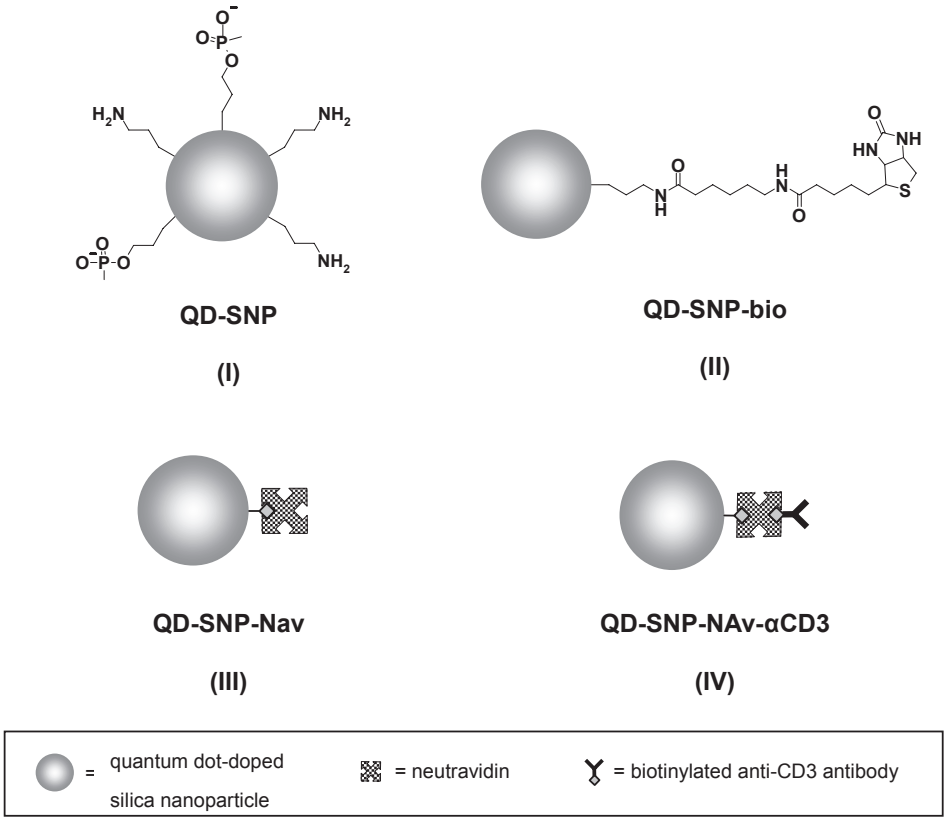

Scheme 1 Quantum dot (QD)-doped silica nanoparticles (SNP) functionalized with amino and phosphonate groups (**I**), after coupling of the QD-SNP amino groups to a biotin-labeling reagent (**II**), decoration of QD-SNP-bio with neutravidin (Nav) (**III**), and after incubation of QD-SNP-Nav with biotinylated mouse anti-human CD3 (**IV**).

5 mg of Nav overnight. The QD-SNP-Nav (Scheme 1[III]) were washed with PBS until the absorbance of the wash at 280 nm demonstrated the absence of protein.

Internalization of QD-SNP-Nav by CD3-mediated endocytosis

QD-SNP-Nav (100 µg) were incubated with biotinylated αCD3 antibody (20 µg) for 1 h (Scheme 1[IV]). The QD-SNP-Nav-αCD3 were washed three times with PBS. Human Jurkat T leukemia cells were grown at 37 °C in 5% CO_2 in RPMI-1640 supplemented with 10% FBS. Cells (10^5) in logarithmic growth were washed with RPMI-1640, resuspended in 0.5 ml of RPMI-1640, incubated with QD-SNP-Nav-αCD3 (7 µg) in PBS (300 µl) for 3 h at 37 °C in 5% CO_2, washed twice in PBS and then incubated for 30 min at 37 °C in 5% CO_2 on poly-L-lysine-coated cover slips. HeLa adenocarcinoma cells were seeded onto cover slips, maintained in logarithmic growth by culture in DMEM-HG for 24 h and then treated with QD-SNP-Nav-αCD3 in PBS for 3 h at 37 °C in 5% CO_2. The cells on the cover slips were fixed for 10 min in 3.7% formaldehyde in PBS, blocked and permeabilized with PBS containing 5% NMS and 0.3% Triton X-100, and then either stained for 1 h at room temperature with 10 µg/ml Texas Red-conjugated concanavalin A, or incubated with rabbit anti-CD107A in PBS containing 3% NMS and 0.1% Triton X-100 followed by staining with Texas Red-labeled goat anti-rabbit antibody in PBS containing 3% NGS and 0.1% Triton X-100. The nucleus was visualized using mounting medium containing DAPI (VECTASHIELD, Vector Laboratories, Inc., Burlingame, CA).

Fluorescent microscopy

Phase-contrast and fluorescence images of functionalized SNP were acquired using an inverted microscope (TE300 Nikon, Kanagawa, Japan). Fluorescent imaging was performed using a confocal microscope (Radiance 2100/AGR-3Q, Bio Rad, Hercules, CA) after excitation either at 488 nm using an argon laser to excite the QD, or at 568 nm using a krypton laser to excite the Texas Red. Both 40× and 60× (1.4-oil immersion) objectives were used. Wet samples were imaged to avoid any fluorescence interference from salt crystals caused by evaporation of buffer.

Transmission electron microscopy

An aliquot (3 µl) of QD-SNP in ethanol was dropped onto lacey carbon film covering a 300-mesh copper grid (Tedpella, Inc., Redding, CA) allowing the ethanol to evaporate. Transmission electron microscopy (TEM) images were obtained using a Hitachi H-600A (Tokyo, Japan).

Results and discussion

Molecular weight estimation of QD-SNP

TEM images of the QD-SNP showed a uniform diameter (20 ± 1 nm) of silica nanoparticles functionalized with 3-aminopropyl and phosphonopropyl groups. Assuming that the density of the SNP was equal to pure silica (1.96 g/cm^3) and that the weight of encapsulated QD was negligible, the weight of one SNP having a 20-nm diameter was calculated ($1.96 \times 4/3\pi r^3$) to be approximately 8.2×10^{-18}g. Therefore, the molecular weight of a QD-SNP was calculated (weight × Avogadro number) as approximately 5×10^6.

Loading of Nav on QD-SNP-Nav

The phosponate groups on the QD-SNP surface facilitated the dispersion of nanoparticles in PBS and the subsequent coupling of the SNP amino groups to the biotin-labeling reagent followed by the decoration of SNP-bio with Nav. The presence of linked Nav on the surface of QD-SNP was initially determined on the basis of the following observation. It has been reported that biotin binding blue-shifts the tryptophan fluorescence emission peak (λ_{max}) and reduces the bandwidth at half height (full-width half-maximum, FWHM) (Kurzban et al 1990). Streptavidin and Nav are tetrameric proteins carrying three tryptophans in each monomer. Upon excitation at 290 nm QD-SNP-Nav dispersion in PBS showed an emission band that was blue-shifted and narrower than that exhibited by free Nav dispersed in PBS (Figure 1 and Table 1). We prepared mixtures having molar ratios between Nav and biotin from 1:1 to 1:4. After 2 hours of incubation, we collected their emission spectra after excitation at 290 nm. The tryptophan fluorescence emission peak was observed to blue-shift and narrow with increasing biotin. Specifically in the case of a Nav:biotin molar ratio equal to 1:2, the emission spectrum resembled that exhibited by QD-SNP-Nav suggesting that each Nav was linked to QD-SNP-bio through approximately 2 biotin molecules.

We recorded the absorbance value at 283 nm of Nav in PBS for several concentrations of the protein and calculated an extinction coefficient of Nav in PBS at 283 nm (ε_{Nav}) equal to approximately 1.1×10^5 M^{-1}cm^{-1}. We subtracted the absorbance spectrum of QD-SNB in PBS from the spectrum of QD-SNB-Nav to obtain the spectrum of Nav linked to QD-SNP. From the value of absorbance at 283 nm of Nav linked to QD-SNP and the previously calculated ε_{Nav} we calculated that approximately 40 proteins were on each SNP.

Spectroscopic characterization of QD-SNP-Nav

For up to several months QD-SNP-Nav in PBS at 4 °C remained as a clear solution without any visible flocculation. Moreover, the QD-SNP-Nav in PBS exhibited intense fluorescence (Figure 2). These results, which suggest that the QD-SNP-Nav was a monodispersed suspension, were confirmed by both optical and confocal microscopy which showed that QD-SNP-Nav in PBS had no distinct fluorescent features (Figure 3). The absorbance spectrum of QD-SNP-Nav in PBS exhibited a blue-shifted band that was broader

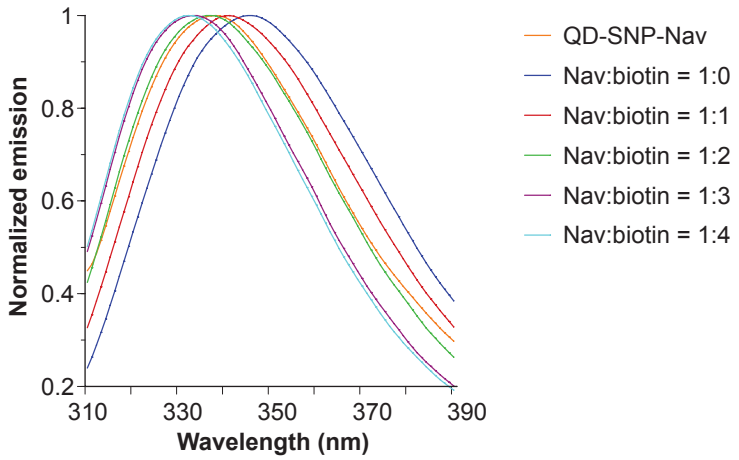

Figure 1 Normalized emission spectra on excitation upon 290 nm for QD-SNP-Nav dispersed in PBS and for mixtures with different molar ratios of Nav and biotin in PBS.
Abbreviations: Nav, neutravidin; PBS, phosphate-buffered saline; QD, quantum dots; SNP, silica nanoparticles.

Table 1 Maximum emission wavelength and full-width half-maximum for QD-SNP-Nav dispersed in PBS and for mixtures with different molar ratios of Nav and biotin in PBS, after excitation at 290 nm

Sample	λ_{max}† (nm)	FWHM‡ (nm)
QD-SNP-Nav	338	60
Nav:biotin = 1:0	346	63
Nav:biotin = 1:1	341	61
Nav:biotin = 1:2	337	59
Nav:biotin = 1:3	333	56
Nav:biotin = 1:4	332	55

Notes: †maximum emission wavelength; ‡full-width half-maximum.
Abbreviations: Nav, neutravidin; PBS, phosphate-buffered saline; QD, quantum dots; SNP, silica nanoparticles.

than the corresponding 531 nm-centered band of QD suspended in toluene (Figure 4A). After excitation at 488 nm, the steady-state emission spectrum of QD-SNP-Nav in PBS exhibited a slightly broader and blue-shifted emission peak compared to that of free QD in toluene (Figure 4B and Table 2). QD are characterized by spectroscopic properties strictly dependent upon their physical dimension. In particular, the maximum in the absorption spectrum (corresponding to the first electronic transition) and the emission peak shift to shorter wavelengths with decreasing size of the nanocrystal. Therefore, the blue-shift of both absorption and emission bands could be explained by considering a decrease of the size of the nanocrystal core due to a partial oxidation of the QD surface during the hydrolysis and condensation of the silica precursor. The broadening of the maximum of the first electronic transition in the absorption spectrum may be due to a change of the refractive index of the medium surrounding the QD after the encapsulation into the silica matrix.

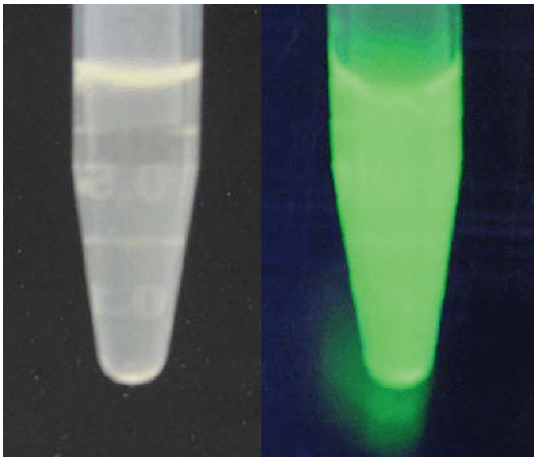

Figure 2 Photographs of QD-SNP-Nav in PBS before (left) and after (right) illumination with 365-nm UV light.
Abbreviations: Nav, neutravidin; PBS, phosphate-buffered saline; QD, quantum dots; SNP, silica nanoparticles; UV, ultraviolet.

Internalization of QD-SNP-Nav by CD3-mediated endocytosis

The transport of various types of proteins that were noncovalently and nonspecifically bound to engineered nanomaterials into various adherent and nonadherent mammalian cell lines by endocytosis has been reported (Kam and Dai 2005). Recently, our group reported the internalization of a carbon nanotube-based supramolecular luminescent nanoassembly by Jurkat cells that had been stimulated with biotinylated αCD3 (Bottini et al 2006a). The decoration of QD-SNP with neutravidin stably solubilized the QD-SNP-Nav under physiological conditions and, therefore, provided a potential scaffold for intracellular transporters. Here, we investigated whether QD-SNP-Nav could be used as a fluorescently detectable intracellular nanoprobe in Jurkat cells through specific CD3 receptor-mediated endocytosis.

QD-SNP-Nav (100 μg, 2×10^{-11} mol of SNP assuming a molecular weight of 5×10^6) were first incubated with biotinylated αCD3 (20 μg, 1.33×10^{-10} mol of antibodies assuming a molecular weight of 1.5×10^5) to introduce αCD3 by binding of its biotin moiety to unoccupied sites on Nav (QD-SNP-Nav-αCD3) and then washed three times with PBS. In this way, we avoided preliminary treatment of cells with antibodies, and were able to obtain improved CD3 binding as compared to the previously published intracellular nanoprobes. We verified the amount of αCD3 linked to the QD-SNP-Nav using polyacrylamide gel electrophoresis and Western immuno-blotting. The fact that the supernatant fraction collected after the first wash did not contain free antibodies suggested that all the antibodies were linked to the Nav on the QD-SNP and, therefore, that approximately 6 αCD3 antibodies were available for each QD-SNP-Nav-αCD3.

Endocytosis is an energy-dependent process with optimum uptake occurring at 37 °C but none occurring at 4 °C. Jurkat cells that were incubated with QD-SNP-Nav-αCD3 at 37 °C had intense internal fluorescence (Figure 5A). To investigate whether internalized QD-SNP-Nav-αCD3 localized in the nucleus, the cells were stained with the

Table 2 Maximum emission wavelength and full-width half-maximum for dipersions of QD in toluene and QD-SNP-Nav in PBS, after excitation at 488 nm

Sample	λ_{max}† (nm)	FWHM‡ (nm)
QD in toluene	542	28
QD-SNP-Nav in PBS	538	32

Note: †maximum emission wavelength; ‡full-width half-maximum.
Abbreviations: FWHM, full-width, half-maximum; Nav, neutravidin; PBS, phosphate-buffered saline; QD, quantum dots; SNP, silica nanoparticles.

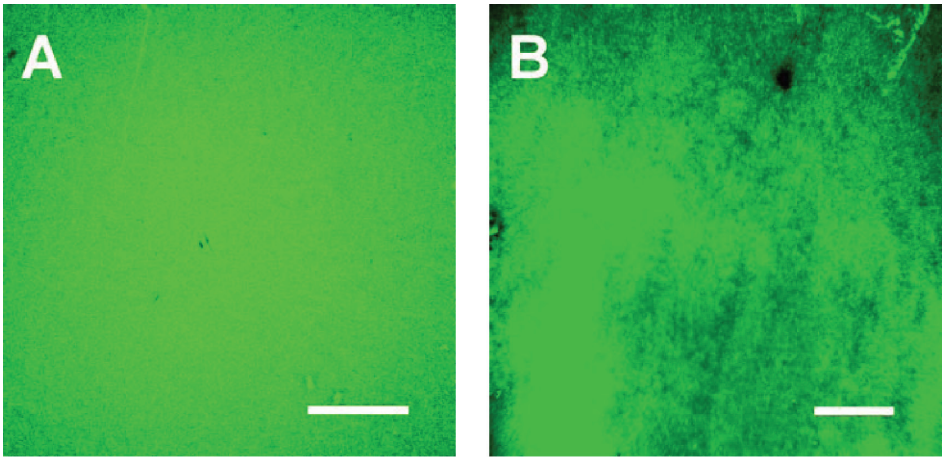

Figure 3 Optical (A) and confocal (B) fluorescent images of QD-SNP-Nav dispersed in PBS. That both fields displayed uniform fluorescence suggests that the nanoassemblies were fully dispersed in PBS (scale bars approximately 10 μm).
Abbreviations: Nav, neutravidin; PBS, phosphate-buffered saline; QD, quantum dots; silica nanoparticles.

nuclear stain DAPI. QD-SNP-Nav-αCD3 fluorescence did not overlap that of DAPI suggesting that, after endocytosis, QD-SNP-Nav-αCD3 was not transported to the nucleus. Furthermore, staining using rabbit anti-CD107A followed by Texas Red-labeled goat anti-rabbit antibody to visualize the lysosomes, the organelles that digest macromolecules, showed that the red (lysosome) and green (QD-SNP-Nav-αCD3) fluorescence overlapped indicating that after cellular uptake some endocytotic vesicles containing QD-SNP-Nav-αCD3 fused with lysosomes (Figure 5B).

Jurkat cells that had been treated with QD-SNP-Nav-αCD3 at 4 °C or those treated with QD-SNP-Nav alone, or those previously incubated with unconjugated αCD3, either at 4 °C or 37 °C, exhibited weak internal fluorescence (Figure 5C). Moreover, only a few adherent HeLa cells, which lack CD3 receptor, incubated with QD-SNP-Nav-αCD3 showed extremely weak internal red fluorescence.

Overall, these results suggest that without stimulation of the Jurkat CD3 membrane receptor (by QD-SNP-Nav alone or in presence of nonconjugated αCD3) or treatment of HeLa cells with QD-SNP-Nav-αCD3 in absence of the CD3 surface receptor the endocytotic uptake of the nanoassembly was weak and most likely due to nonspecific interactions between the nanoassembly and hydrophobic regions of the cell surface. On the other hand, the endocytotic uptake of the QD-SNP-Nav was strongly amplified by specific CD3 receptor-mediated endocytosis with αCD3 crosslinking of the CD3 surface receptor to the nanoassembly through biotin-neutravidin binding. Furthermore, once internalized, some of the nanoassembly colocalized with lysosomes.

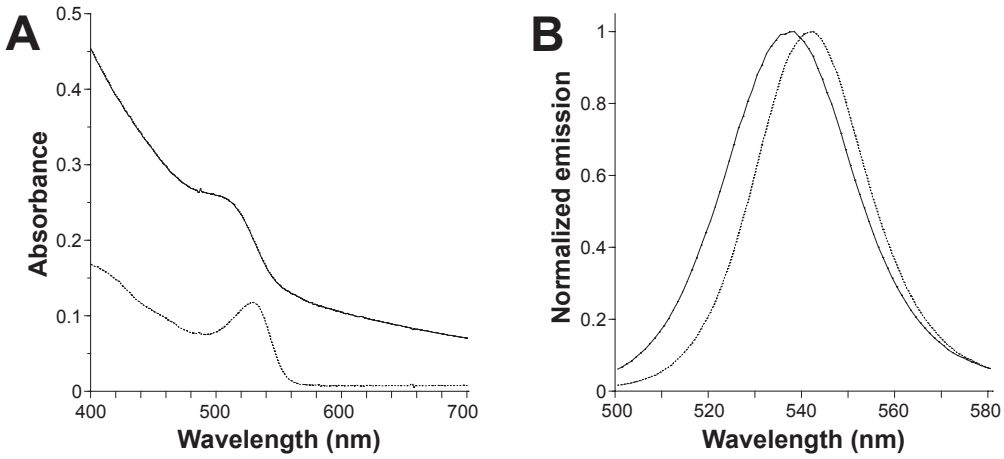

Figure 4 Absorbance (A) and normalized emission (B) spectra of QD in toluene (dotted line) and QD-SNP-Nav dispersed in PBS (solid line).
Abbreviations: Nav, neutravidin; PBS, phosphate-buffered saline; QD, quantum dots; silica nanoparticles.

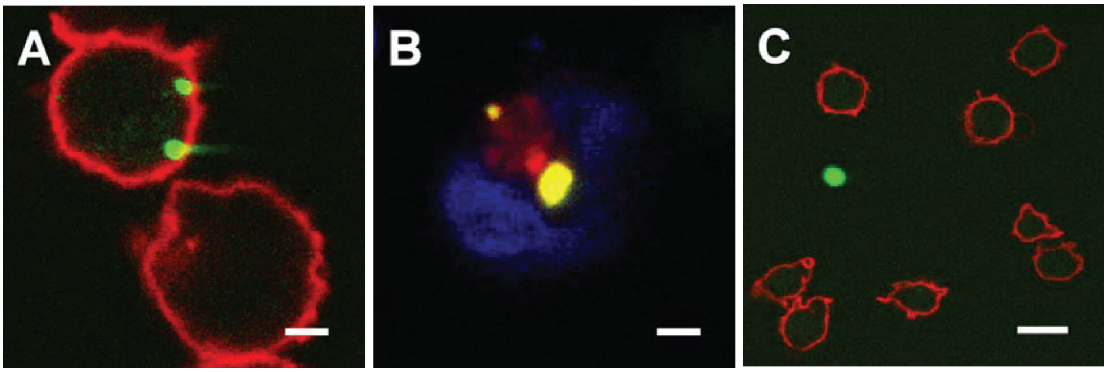

Figure 5 (A) Confocal fluorescent image of QD-SNP-Nav internalized in Jurkat T leukemia cells through specific CD3 receptor-mediated endocytosis (scale bar approximately 2 μm). (B) Confocal fluorescent image of QD-SNP-Nav internalized into Jurkat T leukemia cells incubated with rabbit anti-CD107A and then with Texas Red-labeled goat anti-rabbit antibody in order to visualize lysosomes. The co-localization of intracellular nanoassemblies (green) and lysosomes (red) indicate that after CD3 receptor-mediated endocytotic uptake, part of internalized QD-SNP-Nav were transported to lysosomes (scale bar approximately 1 μm). (C) Confocal fluorescent image of Jurkat cells treated at 37 °C with QD-SNP-Nav previously incubated with unconjugated αCD3 (scale bar approximately 5 μm).
Abbreviations: Nav, neutravidin; PBS, phosphate-buffered saline; QD, quantum dots; silica nanoparticles.

Conclusions

We prepared QD-doped silica nanoparticles coated with neutravidin (QD-SNP-Nav), which were visible by conventional fluorescent microscopy. These nanoassemblies which are able to exploit the strong affinity between a functionalized biotin and neutravidin, and have the potential for further functionalization with macromolecules, nucleic acids, and polymers. This fluorescent nanoassembly was delivered into Jurkat T cells through CD3 receptor-mediated endocytosis and was partially released to lysosomes. In this regard, QD-SNP-Nav represents a potentially useful scaffold for constructing specific intracellular nanoprobes.

In the future we plan to investigate whether QD-SNP-Nav functionalized with a synthetic pH-sensitive polymer can release drug to the cytoplasm compartment or can deliver nucleic acids into a cell.

Acknowledgments

This work was supported by Grant U54 CA119335-02 from the National Institutes of Health. We thank Dr. Nunzio Bottini (University of Southern California, Los Angeles, CA) and Dr. Ana Miletic Sedy (Burnham Institute for Medical Research, La Jolla, CA) for helpful comments.

References

Akerman ME, Chan WC, Laakkonen P, et al. 2002. Nanocrystal targeting in vivo. *Proc Natl Acad Sci U S A*, 99:12617–21.

Bagwe RP, Hilliard LR, Tan W. 2006. Surface modification of silica nanoparticles to reduce aggregation and nonspecific binding. *Langmuir*, 22:4357–62.

Bagwe RP, Yang C, Hilliard LR, et al. 2004. Optimization of dye-doped silica nanoparticles prepared using a reverse microemulsion method. *Langmuir*, 20:8336–42.

Bianco A. 2004. Carbon nanotubes for the delivery of therapeutic molecules. *Expert Opin Drug Deliv*, 1:57–65.

Bottini M, Cerignoli F, Dawson MI, et al. 2006. Full-length single-walled carbon nanotubes decorated with streptavidin-conjugated quantum dots as multivalent intracellular fluorescent nanoprobes. *Biomacromolecules*, 7:2259–63.

Bottini M, Magrini A, Di Venere A, et al. 2006. Synthesis and characterization of supramolecular nanostructures of carbon nanotubes and ruthenium-complex luminophores. *J Nanosci Nanotechnol*, 6:1381–6.

Haag R. 2004. Supramolecular drug-delivery systems based on polymeric core-shell architectures. *Angew Chem Int Ed Engl*, 43:278–82.

Hardman R. 2006. A toxicologic review of quantum dots: toxicity depends on physicochemical and environmental factors. *Environ Health Perspect*, 114:165–72.

Kam NW, Dai H. 2005. Carbon nanotubes as intracellular protein transporters: generality and biological functionality. *J Am Chem Soc*, 127:6021–6.

Kurzban GP, Gitlin G, Bayer EA et al. 1990. Biotin binding changes the conformation and decreases tryptophan accessibility of streptavidin. *J Protein Chem*, 9:673–82.

Langer R, Tirrell DA. 2004. Designing materials for biology and medicine. *Nature*, 428:487–92.

Lin YW, Liu CW, Chang HT. 2006. Synthesis and properties of water-soluble core–shell–shell silica–CdSe/CdS–silica nanoparticles. *J Nanosci Nanotechnol*, 6:1092–1100.

Salem AK, Searson PC, Leong KW. 2003. Multifunctional nanorods for gene delivery. *Nat Mater*, 2:668–71.

Shenoy D, Fu W, Li J, et al. 2006. Surface functionalization of gold nanoparticles using hetero-bifunctional poly(ethylene glycol) spacer for intracellular tracking and delivery. *Int J Nanomedicine*, 1:51–7.

Stöber W, Fink A, Bohn E. 1968. Controlled growth of monodisperse silica spheres in the micron size range. *J Colloid Interface Sci*, 26:62–9.

Wang J, Zhang K, Zhu Y. 2005. Synthesis of SiO_2-coated $ZnMnFe_2O_4$ nanospheres with improved magnetic properties. *J Nanosci Nanotechnol*, 5:772–5.

Zhang T, Stilwell JL, Gerion D, et al. 2006. Cellular effect of high doses of silica-coated quantum dot profiled with high throughput gene expression analysis and high content cellomics measurements. *Nano Lett*, 6:800–8.